COOPERATIVE POLYMERIZATION REACTIONS

Analytical Approximations, Numerical Examples, and Experimental Strategy

ROBERT F. GOLDSTEIN AND LUBERT STRYER
Department of Cell Biology, Sherman Fairchild Center, Stanford University School of Medicine, Stanford, California 94305

ABSTRACT   How does one obtain kinetic rate constants from the time course of a reversible and cooperative polymerization reaction? We examine a simple version of the homogeneous nucleation-elongation model with both analytical and numerical techniques to test some common assumptions and develop an experimental strategy. The assumption of irreversible polymer formation is found to be a useful and adequate approximation for the numerical determination of monomer disappearance. The assumption of early "pre-equilibrium" between monomer and seed, however, is shown numerically and analytically to produce significant errors over a wide range of parameters, particularly for small seed lengths. We exhibit numerical solutions for many different parameters, and also discuss analytical techniques that allow approximate solutions for several conditions: the high-concentration limit; the long-time limit; and the long-seed-length, lows concentration limit. The overall reaction simplifies when the monomer concentration is large. An experimental strategy for elucidating the seed size and the rate constants for polymerization and depolymerization is presented.

INTRODUCTION

The assembly and dissassembly of biological polymers such as actin or tubulin depend upon direct physical interactions between subunits as well as on nucleoside triphosphate hydrolysis and the intervention of regulating proteins. The physical interactions represented by kinetic parameters form a foundation on which to build an understanding of the more complicated control reactions. In principle, these parameters can be obtained from well-defined in vitro experiments involving purified proteins, but as we shall show, the analysis is by no means simple. Our concern here is with such in vitro systems — this work was originally motivated by studies on actin polymerization, but the results are applicable to all homogeneous polymerization processes, be they on biological or synthetic polymers. The fundamental question is, what does one expect to happen during a cooperative polymerization reaction, and how should the data be analyzed to obtain the kinetic parameters?

Analysis of homogeneous polymerization (when nuclei are formed from monomers, and not from external impurities) particularly in regards actin, was pioneered by Oosawa (1, 2) and his collaborators, and extended by others (3, 4). The reader should consult the reviews by Korn (5) and by Frieden (6) for further details, including analysis of experiments on actin. Other aspects of polymerization reactions, particularly for reactions that are non-cooperative or in which the cooperativity varies with polymer length in certain regular ways, or in which

aggregation of long polymers is important, can be traced to analysis of colloid formation (7, 8, 9). The basic equations governing protein polymerization form an infinite interrelated set of nonlinear differential equations that cannot be solved exactly, and simplifying assumptions must be used. Two important assumptions used were (a) polymer formation is irreversible, and (b) the concentrations of polymers shorter than the seed length would rapidly form a "pre-equilibrium" with the monomer concentration. These assumptions together with subsequent analysis lead to the conclusion that the seed size is simply related to a suitably defined "delay time". Indeed, measurements of delay time vs. total protein concentration have been interpreted in terms of explicit seed sizes (10).

Frieden and Goddette (11) have shown by numerical examples, however, that seed size is not simply related to delay times for all parameter regimes. Thus analysis of experiments becomes much more complicated, and Frieden and Goddette advise numerically searching parameter space over a wide range of total protein concentrations in order to fit the data.

Numerical searches can be quite time consuming, particularly when the dimensionality of parameter space can easily be expanded by assigning different rate constants to different polymerization steps. Certain questions arise: Are all simple approximation schemes hopeless, and must one always resort to numerical simulation? Is it possible to derive validity conditions for the various approximations? If the simulated curves don't quite fit the data, is it because the model is wrong, or because parameter space wasn't

explored thoroughly enough? If the model is wrong, can it be fixed by small measures, such as adding an extra rate constant, or should more drastic measures be taken, such as consideration of branching reactions, ATP hydrolysis, etc.? We shall address these questions and propose an analysis of experimental data that is reasonably straightforward, but does not use simplifying assumptions unquestioningly.

This paper is organized as follows. First the model is defined. Then the efficacy of the irreversibility and pre-equilibrium assumptions is examined by using scaling arguments to compare the number concentration of long polymers under long-time, high concentration conditions for three cases: equilibrium, pre-equilibrium plus irreversibility, and irreversibility alone. Although the irreversibility condition produces too many polymers at long times, the extent of the overproduction depends heavily on the pre-equilibrium assumption. This is serious because the concentration of polymers governs the rate of monomer disappearance; as far as monomer disappearance, the pre-equilibrium assumption is certainly not valid under extreme high-concentration conditions.

After this general analysis of assumptions, we exhibit numerical solutions of the exact equations and compare them with numerical solutions of the irreversible equations. This will illustrate quantitatively many of the points made earlier. For example, an assumption of irreversibility, as opposed to high-concentration, holds over the time range of monomer disappearance for a large range of total protein concentrations.

After the numerical results, we return to the analytical analysis in more detail. The exact equations are solved via an integral transform on the time variable in the high concentration limit, and we then apply a perturbation treatment to find appropriate corrections when the concentration is not so high. In particular, this allows the determination of polymerization at early times, and we find it scales as t^s where s is the seed size, but only in certain parameter regimes, contrary to other theories (2, 12) that predict a t^2 dependence.

Once the monomer concentration has equilibrated, the polymer length redistribution obeys linear differential equations. These are solvable, and lead to the relaxation times for long polymers as well as for the monomer. The equations for the long-seed, low-concentration case are also linear (at least at early times), and this can result in validity conditions for establishment of pre-equilibrium between monomer and pre-seeds.

Once our theoretical results have been presented, we shall compare and relate our work to previous studies, and conclude with a strategy for the design of experiments. The discussion of the work of other investigators is placed toward the end of this paper so the results and notation presented here could serve as a common basis of comparison.

Our focus throughout is on a detailed analysis of simple,

cooperative polymerization reactions, including an examination of various approximations and their ranges of validity. Our results allow us to develop an experimental strategy that is discussed in a later section. We had hoped, given our interest in actin assembly, to conclude with a convincing analysis of various actin polymerization experiments. Unfortunately, we know of no data (including our own) that extends over a wide enough concentration range to be amenable to our proposed analysis. An analysis of data that exemplifies our methods will therefore have to wait for the future.

THE MODEL

Consider the simplest model possible for cooperative polymerization. That is, the only reactions allowed are stepwise additions and subtractions of single monomers from only one end of the polymers. Thus, if A_n represents the concentration of polymers of length n, then the reactions are $2A_1 \rightleftharpoons A_2$, $A_1 + A_{n-1} \rightleftharpoons A_n$, ad infinitum. We further assume there exists a unique polymer size, s, such that in the reaction $A_1 + A_n \rightleftharpoons A_{n+1}$, the kinetic constants depend only upon whether $n > s$ or $n < s$. Thus the kinetic constants k_+, k_-, g_+, and g_- are defined by

$$A_1 + A_n \underset{k_-}{\overset{k_+}{\rightleftharpoons}} A_{n+1} \quad n < s \qquad (1a)$$

$$A_1 + A_n \underset{g_-}{\overset{g_+}{\rightleftharpoons}} A_{n+1} \quad n \geq s. \qquad (1b)$$

It is straightforward to write out kinetic equations corresponding to these chemical equations. The central purpose of this paper, then, is to find (approximate) solutions to the following:

$$\frac{dA_1}{dt} = -2k_+ A_1^2 + k_- A_2 + k_- \sum_{n=2}^{s} A_n$$
$$+ g_- \sum_{n=s+1}^{\infty} A_n - k_+ A_1 \sum_{n=2}^{s-1} A_n - g_+ A_1 \sum_{n=s}^{\infty} A_n \quad (2a)$$

$$\frac{dA_n}{dt} = k_+ A_1 (A_{n-1} - A_n) + k_- (A_{n+1} - A_n) \quad n < s \quad (2b)$$

$$\frac{dA_s}{dt} = A_1 (k_+ A_{s-1} - g_+ A_s) + g_- A_{s+1} - k_- A_s \quad (2c)$$

$$\frac{dA_n}{dt} = g_+ A_1 (A_{n-1} - A_n) + g_- (A_{n+1} - A_n) \quad n > s. \quad (2d)$$

Here the term "seed size" means the length s, where the kinetic constants change, as in Eqs. 1. It should be noted that not all workers use this definition. Others (3, 10, 12) have defined the seed as the smallest length such that addition to the seed is more likely than subtraction from it. With their definition, the length of the the seed may depend on the monomer concentration at any given time, but our definition is independent of time and initial conditions.

We define the equilibrium constants $K_a = k_+/k_-$ and $K_b = g_+/g_-$, and the dimensionless ratios $h_+ = k_+/g_+$ and $h_- = k_-/g_-$. The basic equations can now be transformed into dimensionless quantities defined by $\alpha_n = K_b A_n$ and $\tau = g_- t$:

$$\frac{d\alpha_1}{d\tau} = -2h_+\alpha_1^2 + h_-\alpha_2 + h_-\sum_{n-2}^{s}\alpha_n$$
$$+ \sum_{n-s+1}^{\infty}\alpha_n - h_+\alpha_1\sum_{n-2}^{s-1}\alpha_n - \alpha_1\sum_{n-s}^{\infty}\alpha_n \quad (3a)$$

$$\frac{d\alpha_n}{d\tau} = h_+\alpha_1(\alpha_{n-1} - \alpha_n) + h_-(\alpha_{n+1} - \alpha_n) \quad n < s \quad (3b)$$

$$\frac{d\alpha_s}{d\tau} = \alpha_1(h_+\alpha_{s-1} - \alpha_s) + \alpha_{s+1} - h_-\alpha_s \quad (3c)$$

$$\frac{d\alpha_n}{d\tau} = \alpha_1(\alpha_{n-1} - \alpha_n) + (\alpha_{n+1} - \alpha_n) \quad n > s. \quad (3d)$$

Thus all concentrations are measured in units of the so-called "critical concentration", K_b^{-1}, and all times are measured in units of g_-^{-1}. We shall also designate the cooperativity as $\sigma = h_+/h_- = K_a/K_b$. That is, $\sigma \sim 0$ implies a highly cooperative reaction, and $\sigma \sim 1$ implies almost no cooperativity. $\sigma > 1$ would represent an anti-cooperative reaction, and will not be considered here. σ is directly related to the free energy difference between the $\alpha_{s-1} + \alpha_1 \rightleftharpoons \alpha_s$ reaction and the $\alpha_s + \alpha_1 \rightleftharpoons \alpha_{s+1}$ reaction, i.e. $\Delta G_0 = RT \ln \sigma$.

This expression in dimensionless quantities clearly shows that polymerization reactions are characterized by three dimensionless parameters, in addition to the two scales of time and concentration. These parameters are the seed, s, the cooperativity, σ, and h_+. σ affects mainly equilibrium conditions, and has almost no effect on monomer disappearance at very high monomer concentrations. h_+, on the other hand, is strictly a kinetic parameter, and does not directly affect the equilibrium. One could think of h_+ as the kinetic cooperativity, different from σ, the thermodynamic cooperativity.

The only other parameters are the initial conditions, and unless specified otherwise, we assume that only the monomer is populated at $\tau = 0$. Thus $\alpha_1(0) = \alpha_T$ and $\alpha_n(0)$ or $n \neq 1$, where α_T represents the concentration of total material.

EQUILIBRIUM

One can easily verify by direct substitution that the following functions for α_n are stationary, and therefore represent equilibrium (since no energy is dissipated in our model)

$$\alpha_n = \sigma^{n-1}\alpha_1^n \quad n \leq s \quad (4a)$$

$$\alpha_n = \sigma^{s-1}\alpha_1^n \quad n \geq s. \quad (4a)$$

From Eqs. 4, we calculate the total number of polymers and their average length as follows. The total number concentration, $C = \sum_{n-s+1}^{\infty}\alpha_n$, is given in equilibrium by

$$C_{eq} = \sigma^{s-1}\alpha_1^{s+1}/(1 - \alpha_1), \quad (5)$$

and the equilibrium concentration of monomer is related to the total concentration of material by

$$\alpha_T = \sum_{n-1}^{\infty} n\alpha_n = \frac{s\alpha_1^s\sigma^{s-1}}{1 - \alpha_1} + \frac{\alpha_1^{s+1}\sigma^{s-1}}{(1 - \alpha_1)^2}$$
$$+ \frac{\alpha_1[s(\sigma\alpha_1)^{s-1} - 1]}{\sigma\alpha_1 - 1} - \frac{\sigma\alpha_1^2[(\sigma\alpha_1)^{s-1} - 1]}{(\sigma\alpha_1 - 1)^2}. \quad (6)$$

The dependence of the concentration of polymerized material, $\alpha_T - \alpha_1$, vs. the total material, α_T, is shown in Fig. 1 for different values of s and σ. Note that the differences
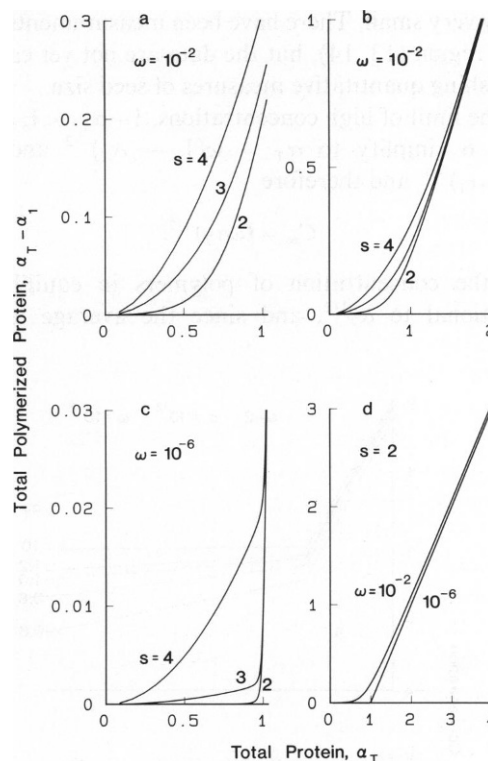

FIGURE 1 Equilibrium—total polymerized monomer ($\alpha_T - \alpha_1$) vs. total protein (α_T) for seeds of 2, 3, 4, and $\omega = \sigma^{s-1}$ values of 10^{-2} and 10^{-6}. (a) $\omega = 10^{-2}$. Note the substantial amount of polymerized monomer ($\approx 20\%$) in the region where $\alpha_T < 1$, i.e. where the total material is less than the critical concentration. (b) Same as a, but with extended scales. Note that for a given ω, the differences between seed sizes rapidly diminish for $\alpha_T > 1$. (c) $\omega = 10^{-6}$. The cooperativity is much higher, and the differences between seed lengths is much lower ($\approx 1\%$) than in a. (d) A comparison of the seed = 2 curves from a and c on an expanded scale. Although curves of equal ω coalesce quickly for $\alpha_T > 1$, curves of unequal ω coalesce much more slowly. This observation is important because the critical concentration is often determined by extrapolating back to the x-intercept from large values of α_T. As can be seen from this figure, if the values of α_T are not large enough, the apparent x-intercept will miss the critical concentration and therefore produce a systematic error. This size of this error depends on ω, which is usually not known a priori.

between curves depend mostly on σ^{s-1}, and only to a lesser extent on s and σ independently. This is because most of the material appears in the long polymers, whose concentration depends on the amount of cooperativity "accumulated" by the seed — if a factor of σ is accumulated for each step before the seed, then we define the cumulative cooperativity, ω, as $\omega = \sigma^{s-1}$. That the equilibrium solutions depend mostly on ω is reinforced by Fig. 2, which shows the equilibrium length distributions for seeds of 2 and 3 in which $\omega = 10^{-2}$. Note that the post-seed slope is similar for curves of similar α_T but different seed size. This is a property of systems having identical ω.

It would thus be very difficult to measure the seed length from equilibrium measurements of the monomer concentration. The differences show up only when the total material is close to but less than the critical concentration, a region in which the number of polymerized monomers is usually very small. There have been measurements of actin in this region (13, 14), but the data are not yet capable of establishing quantitative measures of seed size.

In the limit of high concentrations, $1 - \alpha_1 << 1$, and Eqs. 5 and 6 simplify to $\alpha_T = \omega(1 - \alpha_1)^{-2}$ and $C_{eq} = \omega(1 - \alpha_1)^{-1}$ and therefore

$$C_{eq} = (\omega\alpha_T)^{1/2}. \tag{7}$$

Thus the concentration of polymers in equilibrium is proportional to $\alpha_T^{1/2}$, and since the average length of

FIGURE 2 Equilibrium length distributions for $\omega = \sigma^{s-1} = 10^{-2}$, and α_T = 0.6, 0.8, 1.0, 1.2, 10.0, as labeled. (a) seed = 2. (b) seed = 3. Since these distributions have equal ω values, they differ primarily in the pre-seed lengths, and are quite similar in the long polymer distribution. This underscores the importance of the parameter ω used in Fig. 1.

polymers is α_T/C_{eq}, the average length becomes $(\alpha_T/\omega)^{1/2}$.

These results are valid only in true equilibrium and are presented for contrast with results from kinetic analyses presented next. As Oosawa (15) has shown, the time scale for relaxation of monomer concentration is very different (and much shorter) than the relaxation of the long polymer length distribution. Eqs. 4 apply after the long polymers have reached equilibrium, but the kinetic analyses, at least at high concentration, apply only over the time range of monomer concentration relaxation.

SCALING ARGUMENTS AT HIGH CONCENTRATION

Pre-Equilibrium and Irreversibility

Eqs. 3 form an infinite set of interrelated nonlinear differential equations that cannot, in general, be solved analytically without some approximation. One approach (10) is to assume (a) the monomer concentration changes only by addition to and subtraction from polymers longer than the seed, (b) polymer formation by seed production is irreversible, and (c) the ratio of the concentration of the seed-minus-one-length to the $s - 1$ power of monomer concentration is essentially constant through most of the reaction; that is, the seed precursor is in "pre-equilibrium" with the monomer. (This is the same analytical form as obtained between the seed precursor and monomer in the true equilibrium Eqs. 4). These assumptions allow the infinite set of equations to be reduced to two. Assumption a is

$$\frac{d\alpha_1}{d\tau} = C - C\alpha_1. \tag{8}$$

We take assumption b to mean that

$$\frac{dC}{d\tau} = \alpha_{s-1}(\alpha_1 - 1). \tag{9}$$

(The factor $(\alpha_1 - 1)$ is used instead of α_1 so that polymer formation stops when α_1 reaches the critical concentration. This extra assumption will not affect the analysis below, but is taken into account explicitly in Appendix A). Assumption c implies that

$$\alpha_{s-1} = K\alpha_1^{s-1} \tag{10}$$

and together with assumption b, we have

$$\frac{dC}{d\tau} = K\alpha_1^{s-1}(\alpha_1 - 1). \tag{11}$$

The value of K is usually taken from equilibrium constants, but its exact value is immaterial for our discussion. What matters is that in Eq. 11, α_1 appears with an exponent that depends on seed size. Note that these equations are in dimensionless form, and therefore rate constants such as g_- and g_+ appear implicitly in the definition of α, but not explicitly in Eqs. 8 and 9.
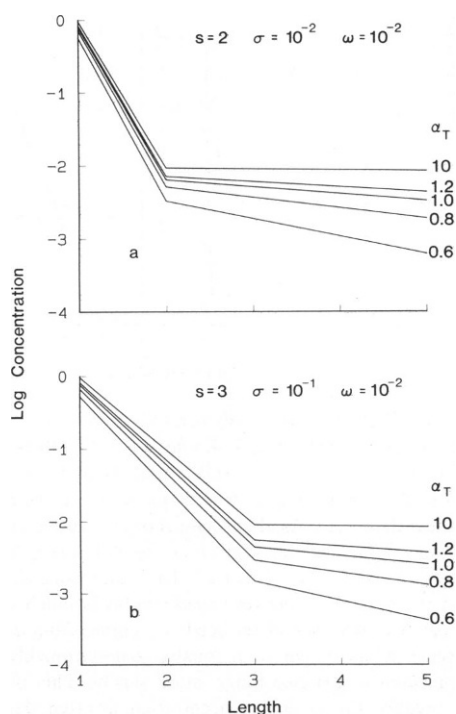
These two equations still cannot be solved exactly but are considerably more tractable than the original infinite set. α_T does not appear in Eqs. 8 and 9, but of course appears in the boundary conditions as $\alpha_1(\tau = 0) = \alpha_T$. We begin analysis of these equations (in the high concentration limit) by considering a transformation of variables that leaves Eqs. 8 and 11 invariant, but removes the α_T dependence from the boundary conditions. This transformation is

$$\alpha_1' = \alpha_1/\alpha_T \tag{12a}$$

$$C' = C/\alpha_T^{s/2} \tag{12b}$$

$$t' = \tau\alpha_T^{s/2}. \tag{12c}$$

Thus in the high concentration limit ($\alpha_1 \gg 1$), the pre-equilibrium/irreversible equations become

$$\frac{d\alpha_1'}{dt'} = -C'\alpha_1', \tag{13a}$$

$$\frac{dC'}{dt'} = K(\alpha_1')^s, \tag{13b}$$

and the boundary conditions become α_1' ($t' = 0$) $= 1$ and $C'(t' = 0) = 0$. Thus in the high concentration limit, α_1 and C' depend only on t' and K, but not on α_T. Even though the equations have not been solved, the entire dependence of α_1 and C on α_T can be exhibited by transforming back to the unprimed representation

$$\alpha_1 = \alpha_T f(\alpha_T^{s/2}\tau), \tag{14a}$$

$$C = \alpha_T^{s/2} F(\alpha_T^{s/2}\tau), \tag{14b}$$

where the functions $f(\ )$ and $F(\ )$ are undetermined and arise from solution of Eqs. 13. We now draw two conclusions from this result.

(a) At $\tau \to \infty$ $F(\ )$ becomes constant, and therefore C ($\tau = \infty$) is proportional to $\alpha_T^{s/2}$. In fact, C ($\tau = \infty$) can be found directly from Eqs. 8 and 11 without assuming the high concentration limit (see Appendix A). The result is C ($\tau = \infty$) $= (2K(\alpha_T^s - 1)/s)^{1/2}$. The dependence on α_T is quite different from the result of the equilibrium calculation, Eq. 7. That these approximate equations should produce too many polymers in equilibrium is due to irreversibility (and not to the high concentration limit, as shown in Appendix A), but the extent of overproduction depends heavily on the pre-equilibrium assumption. Even when one interprets C ($\tau = \infty$) as the total number of polymers after monomer relaxation but before polymer length redistribution, the extent of overproduction is too large. We will verify this assertion in the next section with a similar calculation on irreversible equations without the pre-equilibrium condition. (b) A delay time τ_D can be defined as the time it takes the monomer concentration to reach some arbitrary fraction of its initial value. From Eq. 12c, time (that is, the dimensionless time variable, τ) scales as $\alpha_T^{-s/2}$, and therefore no matter what arbitrary fraction is

chosen,

$$\frac{d \log \tau_D}{d \log \alpha_T} = -\frac{s}{2}. \tag{15}$$

The reason this result is related to the α_T dependence of C ($\tau = \infty$) can be seen in Eq. 8. Roughly speaking, C (τ) is the instantaneous rate constant for monomer decay. Even though C depends on time, C scales with $\alpha_T^{s/2}$ and so will the time dependence of monomer disappearance. This conclusion can be verified by linearizing Eqs. 8 and 11 about their $\tau \to \infty$ point, and will also be seen in the next section with a different version of the polymerization equations.

By using the assumptions of pre-equilibrium and irreversibility, we have found the dependence of the total number of polymers on α_T, and the dependence of the delay time on α_T. In the next section, we shall find different results for these relations when only the irreversibility assumption is used, thus casting doubt on the pre-equilibrium assumption.

Irreversible Polymerization

Consider the Eqs. 3 in the limit in which the monomer concentration is so high that one can ignore all depolymerization reactions. In this case, the equations all have the same basic form

$$\frac{d\alpha_n}{d\tau} = \sum_m \{\text{coefficients}\} \, \alpha_1\alpha_m. \tag{16}$$

That is, the time derivative of each α_n equals a sum of terms, each term of which is quadratic in the α's. In the spirit of Eq. 12, we apply a transformation to remove all α_T dependence from Eqs. 16 and from their boundary conditions. Since Eqs. 16 are of a different form from Eqs. 8–11, we use a different transformation

$$\alpha_n' = \alpha_n/\alpha_T \tag{17a}$$

for all lengths n, and

$$t' = \tau\alpha_T. \tag{17b}$$

By an analogous argument to the one for the pre-equilibrium equations, we draw two analogous conclusions:

(a) Since $C = \sum_{n-s+1}^{\infty} \alpha_n$, and α_n is proportional to α_T for all n, then C ($\tau = \infty$) is proportional to α_T.

(b) Time scales as α_T^{-1}, and therefore $d \log \tau_D/d \log \alpha_T = -1$. Again we note the relation between the delay time and C ($\tau = \infty$), and the fact that irreversibility produces more polymers at $\tau = \infty$ than allowed for by the equilibrium calculation.

There are now three different predictions for the dependence of C ($\tau = \infty$) on α_T in the $\alpha_1 \gg 1$ limit; these come from the true equilibrium equations, from the pre-equilibrium/irreversibility assumptions, and from the true kinetic equations. Due to the apparent relation between C ($\tau = \infty$)

and d log τ_D/d log α_T, one might expect that by linearizing Eqs. 3 about the true equilibrium given by Eqs. 4, the true value for τ_D would be different from that predicted by either the irreversibility assumption alone or from that predicted by the pre-equilibrium and irreversibility assumptions together. The implication is that, insofar as $\alpha_1(\tau)$ is concerned, irreversibility is an unjustified assumption.

We have checked this implication by comparing numerical solutions of the exact Eqs. 3 with the same equations in which irreversibility is assured by preventing only the $A_{s+1} \rightarrow A_1 + A_s$ depolymerization reaction from occurring. In this case, the irreversible polymerization scheme can be written

$$\frac{d\alpha_1}{d\tau} = -2h_+\alpha_1^2 - h_+\alpha_1 \sum_{n=2}^{s-1} \alpha_n$$

$$+ h_- \sum_{n=2}^{s} \alpha_n - \alpha_1\alpha_s + h_-\alpha_2 + (1 - \alpha_1)C \quad (18a)$$

$$\frac{d\alpha_n}{d\tau} = h_+\alpha_1(\alpha_{n-1} - \alpha_n) + h_-(\alpha_{n+1} - \alpha_n) \quad 2 \le n < s \quad (18b)$$

$$\frac{d\alpha_s}{d\tau} = h_+\alpha_1\alpha_{s-1} - \alpha_s\alpha_1 - h_-\alpha_s \quad (18c)$$

$$\frac{dC}{d\tau} = \alpha_1\alpha_s. \quad (18d)$$

Fig. 3 shows this irreversible reaction scheme forms an excellent approximation for monomer decay, not at all in accord with the above reasoning! As mentioned earlier, the explanation is provided by Oosawa's (15) observation that there exist two distinct time scales for polymerization. The first, short time scale governs the disappearance of monomer, but the polymer length distribution relaxes to equilibrium (given by Eqs. 4) over the second, much longer time scale. According to our simulations, the total number of polymers relaxes over the longer time scale — by the time the monomer reaches its equilibrium concentration, the number of polymers may be orders of magnitude larger than will be obtained at true equilibrium. After monomer decay, most of the polymers must therefore depolymerize entirely back to monomer so as to elongate the few polymers that remain. During this process, the monomer concentration stays essentially constant, but there is a large flux of material through the monomer stage.

In summary, we have shown that the assumption of irreversible polymerization is justified over the time course of monomer disappearance, but fails at longer times by predicting too many polymers in equilibrium. The extent of polymer overproduction, however, depends on the validity of the pre-equilibrium assumption. Our analysis shows, at least at high concentration, that the pre-equilibrium assumption must break down, and the relation between delay time and total protein becomes independent of the seed size. We show later that under some conditions, the
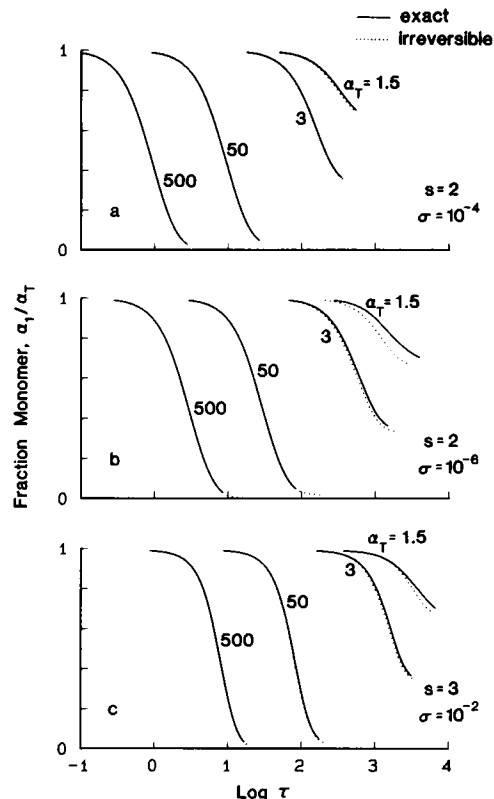

FIGURE 3 Fraction monomer (α_1/α_T) vs. log τ, as calculated with the irreversible approximation Eqs. 18 (dotted line) and with the exact Eqs. 3 using a maximum polymer length of 1,000 to 3,000 (solid line). Each panel shows $\alpha_T = 500, 50, 3$, and 1.5, as labeled. (a) seed $= 2$, $h_+ = 10^{-6}$, $h_- = 1.0$. (b) seed $= 2$, $h_+ = 10^{-5}$, $h_- = 10^{-1}$. (c) seed $= 3$, $h_+ = 10^{-3}$, $h_- = 10^{-5}$. In general, the assumption of irreversible polymerization is an excellent approximation, and starts to fail only for very low concentrations and long times. Of course, it is inappropriate for describing the relaxation of the long polymer length distribution after $\alpha_1 = 1$, even if the starting concentration is high.

pre-equilibrium assumption does not seem to be valid at any concentration, whereas under other conditions, notably large seed size, the pre-equilibrium assumption may be valid at low concentrations. Thus one should be wary of using Eq. 15 to determine the seed size without being assured that pre-equilibrium holds under the relevant conditions.

NUMERICAL EXAMPLES

In addition to comparing solutions for monomer decay for the exact (Eqs. 3) and irreversible (Eqs. 18) calculations in Fig. 3, we have also calculated the time dependence of the entire length distribution for three sets of parameters, as seen in Figs. 4–6. These calculations were performed with the exact set of equations, since although the monomer concentration is accurately predicted by the irreversible approximation, all information about the distribution of long polymers is lost. The calculations here are intended to give a qualitative feeling for what actually happens to all components during a polymerization reaction.
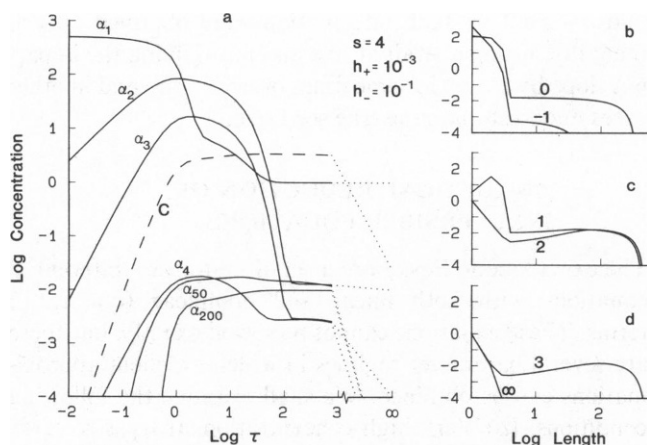
FIGURE 4 Time course of polymer concentrations for $s = 4$, $h_+ = 10^{-3}$, $h_- = 10^{-1}$, $\alpha_T = 500$. (a) Solid line: $\log\alpha_n(\tau)$ vs. $\log\tau$ for $n = 1, 2, 3, 4, 50, 200$. Dashed line: $\log C(\tau)$ vs. $\log\tau$. (b), (c), (d) Same calculation as in a but plotted as $\log\alpha_n(\tau)$ vs. $\log n$. Each curve is labeled by an approximate $\log\tau$. The exact values are: (b) $\tau = 0.1, 1.1$; (c) $\tau = 12, 96$; (d) $\tau = 730, \infty$.

Note in Fig. 4 that the dimer and trimer and even the tetramer (seed) increase over most of the time range when the monomer decreases. Thus "pre-equilibrium" conditions certainly do not apply. In fact, the dimer and trimer concentrations even surpass the monomer concentration during part of the time range and end up overshooting their equilibrium concentrations by several orders of magnitude.

We expect the irreversible approximation to hold over the early part of the polymerization, and thus h_- will not affect the early part of the reaction. It does, however, affect the final equilibrium concentrations, so that the concentration overshoot is the result of interplay between h_+, which governs the peak concentration, and $\sigma = h_+/h_-$ which governs the final equilibrium.
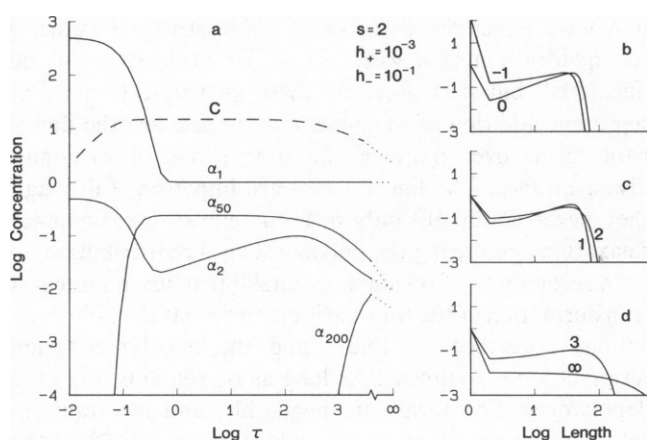

FIGURE 5 Time course of polymer concentrations for $s = 2$, $h_+ = 10^{-3}$, $h_- = 10^{-1}$, $\alpha_T = 500$. (a) Solid line: $\log\alpha_n(\tau)$ vs. $\log\tau$ for $n = 1, 2, 50, 200$. Dashed line: $\log C(\tau)$ vs. $\log\tau$. (b), (c), (d) Same calculation as in a but plotted as $\log\alpha_n(\tau)$ vs. $\log n$. Each curve is labeled by an approximate $\log\tau$. The exact values are: (b) $\tau = 0.1, 1$; (c) $\tau = 12, 96$; (d) $\tau = 1,020, \infty$.
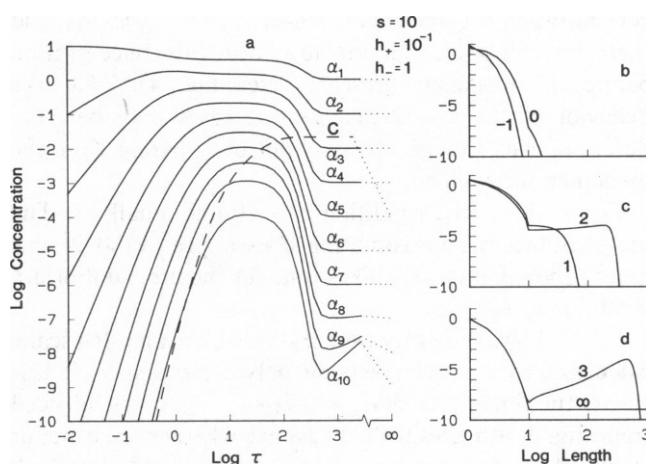

FIGURE 6 Time course of polymer concentrations for $s = 10$, $h_+ = 10^{-1}$, $h_- = 1$, $\alpha_T = 10$. (a) Solid line: $\log\alpha_n(\tau)$ vs. $\log\tau$ for $n = 1, 2, 3, 4, 5, 6, 7, 8, 9, 10$. Dashed line: $\log C(\tau)$ vs. $\log\tau$. (b), (c), (d) Same calculation as in a but plotted as $\log\alpha_n(\tau)$ vs. $\log n$. Each curve is labeled by an approximate $\log\tau$. The exact values are: (b) $\tau = 0.095, 1.1$; (c) $\tau = 12, 92.5$; (d) $\tau = 980, \infty$.

Once the monomer concentration drops close to $\alpha_1 = 1$, the dimer and trimer concentrations relax principally by monomer subtraction, a linear process with a rate constant of h_-. This decay of pre-seeds with an h_- time scale is clear in Fig. 4.

Fig. 5 shows the same h_+, h_-, and α_T as Fig. 4, but the seed has been changed to $s = 2$. Therefore the cooperativity, σ, remains the same, but the cumulative cooperativity, $\omega = \sigma^{s-1}$ is changed. Again, we note that h_- does not affect the early reaction course. Remarkably, the dimer time course is quite different between $s = 4$ and $s = 2$. For a seed length of 2 the dimer concentration seems to parallel the monomer concentration, although at reduced amplitude, and its time derivative shows several sign reversals. Note this is not a true "pre-equilibrium" as discussed earlier, because α_2 scales approximately as $\alpha_1^{1/2}$, not as α_1^2.

A seed of two appears to be a special one for the following reason. One can identify three special polymer lengths: (a) the monomer, because it directly interacts with all lengths and because it is usually in very high concentration at the beginning of the reaction; (b) the seed, because the kinetic constants change at that length; (c) the dimer, because it grows via a term quadratic in α_1 while all other polymers grow by terms linear in α_1—that is, the dimer is more strongly coupled to the monomer than is any other polymer length. Thus when the dimer and seed coincide, there is no pre-seed to buffer the effects of the monomer. In the early stages of the reaction, if $d\alpha_2/d\tau$ is not too large, then the dimer concentration is governed by creation from the monomer and elongation to the trimer; from Eq. 3c we then see that $\alpha_2 \approx h_+\alpha_1$, near $\tau = 0$, which appears correct in Fig. 5. If the seed were not two, however, the decay from dimer to monomer may more effectively compete with the slower elongation to trimer. Also, the "early", or peak, α_2

concentration becomes much larger, $\alpha_2 \approx (h_+/h_-)\alpha_1$, and there may not be enough time to achieve this concentration before the monomer decreases (see Fig. 4). Thus the behavior of the $s = 2$ and $s \neq 2$ cases may be quite different, even though this may not be apparent from the monomer decay alone.

Fig. 6 shows the condition $s = 10$ and small α_T. The pre-equilibrium approximation does appear valid in this case, although it clearly takes time for the pre-equilibrium condition to develop.

Fig. 7 shows the delay time, τ_D, vs. α_T on a log-log scale, calculated assuming irreversible polymerization. τ_D in this case is the time to reach $\alpha_1 = 0.7(\alpha_T - 1)$. (As evidenced from Fig. 3, it makes little difference whether the exact or irreversible equations are used). As expected, the high concentration slope is -1, independent of seed. The slopes at lower concentrations depend on seed size and on h_+, h_-.

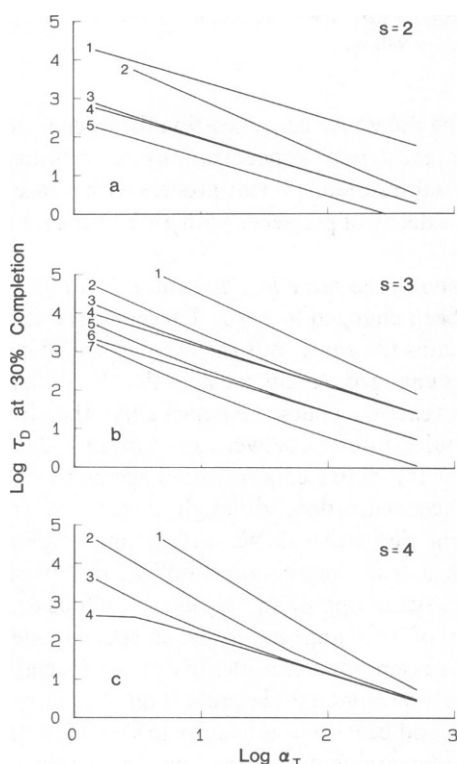

FIGURE 7 Log delay time (measured in dimensionless time, τ), evaluated at 30% polymerization, i.e. when $\alpha_1 = 0.7(\alpha_T - 1)$ vs. log α_T for the following choices of parameters: (a) Seed = 2. Curve 1: $h_+ = 10^{-9}, h_- = 10^{-3}$. Curve 2: $h_+ = 10^{-6}, h_- = 10^3$. Curve 3: $h_+ = 10^{-6}, h_- = 10^0$. Curve 4: $h_+ = 10^{-6}, h_- = 10^{-3}$. Curve 5: $h_+ = 10^{-5}, h_- = 10^{-3}$. (b) Seed = 3. Curve 1: $h_+ = 10^{-6}, h_- = 10^0$. Curve 2: $h_+ = 10^{-6}, h_- = 10^{-2}$. Curve 3: $h_+ = 10^{-6}, h_- = 10^{-3}$. Curve 4: $h_+ = 10^{-6}, h_- = 10^{-4}$. Curve 5: $h_+ = 10^{-5}, h_- = 10^{-2}$. Curve 6: $h_+ = 10^{-5}, h_- = 10^{-3}$. Curve 7: $h_+ = 10^{-4}, h_- = 10^{-1}$. (c) Seed = 4. Curve 1: $h_+ = 10^{-4}, h_- = 10^0$. Curve 2: $h_+ = 10^{-4}, h_- = 10^{-1}$. Curve 3: $h_+ = 10^{-4}, h_- = 10^{-2}$. Curve 4: $h_+ = 10^{-4}, h_- = 10^{-3}$. The values of h_+ and h_- are indicated on the figure. At high α_T values, note that the slopes all tend to -1, independent of seed, and that the actual delay time values become independent of h_-. Since the slopes at low α_T may have a wide range of values, depending on h_+ and h_-, any determination of seed size from the slopes of this figure is perilous without a priori knowledge of h_+ and h_-.

and α_T itself. If such information were obtained experimentally, fitting a straight line and multiplying the apparent slope by 2 may in some cases overestimate and in other cases underestimate the true seed size.

ANALYTICAL REDUCTION OF IRREVERSIBLE EQUATIONS

The exact kinetic Eqs. 3 are a set of first-order differential equations with both linear and nonlinear (quadratic) terms. These equations cannot be solved exactly, but there are several parameter regimes in which excellent approximations can be obtained. We shall examine the following conditions: (a) Very high concentration. If α_1 is so large that the addition reactions dominate the subtraction reactions, then only the quadratic terms need be kept. (b) Somewhat high concentration. The calculation at very high concentration can be extended to lower concentrations by perturbative techniques. These corrections supply validity conditions for the high concentration assumption. (c) Long time. After enough time, $\alpha_1 \approx 1$, and all quadratic terms become linear. This approximation is useful in understanding the polymer length redistribution process after the monomer has equilibrated. (d) Long seed, short time, low concentration. If the seed is very long, then at early times the evolution of pre-seeds is (I) linear because the monomer concentration is not changing, and (II) mathematically isomorphic to the long time condition when $s = 1$. This condition allows a calculation of the time needed to establish pre-equilibrium among the pre-seeds, and therefore can be used to derive validity conditions for the pre-equilibrium assumption.

High Concentration

During the monomer relaxation, we shall assume that $\alpha_1 >> 1$ and that the polymerization (quadratic) terms dominate the depolymerization (linear) terms. The relaxation of monomer concentration would be straightforward if the quadratic terms were absent or at least could be linearized, but it is precisely these quadratic terms that represent addition of monomers, and these are the dominant terms over most of the time range of monomer disappearance. The linear terms are important (although they never dominate) only near the end of the monomer relaxation and during the polymer length redistribution.

In recognition of this fact, we shall introduce an integral transformation of the time variable such that the polymerization terms become linear and the depolymerization terms become nonlinear. As long as α_1 remains large the depolymerization terms are negligible, and the resulting set of linear equations can be solved exactly. Despite the appeal of such a solution, the inverse transformation back to real time cannot be done exactly, although approximations are readily available, and are particularly easy at very early times. Nevertheless, this type of solution is useful as an adjunct to the numerical solutions presented earlier

because

(*a*) In the high concentration limit, all terms involving h_- are neglected, and therefore the reaction depends on only two parameters, s and h_+, not on three. Thus one may be more confident of data analysis in this region, since the theoretical model is simpler and more directly related to the data.

(*b*) Departures from the extreme high concentration limit can be found perturbatively.

(*c*) Validity conditions can be derived for the scaling arguments presented above.

(*d*) The solutions might form the basis for more complicated models, such as those involving energy dissipation (ATP hydrolysis, for example), heterogeneous nucleation, branching reactions, fragmentation reactions, etc.

(*e*) The dependence of the delay time τ_D on parameters other than α_T, such as s and h_+, can be obtained and used in analysis of experiments.

(*f*) The early time dependence of polymerization can be shown to scale as t^s when $h_+^{1/s} << 1$, but not otherwise. (The $s = 1$ case can in fact be solved (9) by a different transformation that eliminates the time variable altogether, but the inverse transformation must also be done numerically.)

The derivation of the time-transformation and high-concentration solution is given in Appendix B; here we quote the results. The time transformation is defined as

$$\tau' = \int_0^\tau \alpha_1(t_0)dt_0. \tag{19}$$

We define β_n as

$$\beta_n(\tau') = \alpha_n(\tau) \tag{20}$$

and therefore

$$\tau = \int_0^{\tau'} \frac{dt_0}{\beta_1(t_0)}. \tag{21}$$

From Appendix B, we find that if $h_+ < 1$,

$$\beta_1(\tau') = \sum_{l=1}^{s} \frac{\alpha_T}{s} [1 - h_+(h_+^{s-1} - h_+^s)^{-1/s}e^{-i\pi(2l+1)/s}]$$

$$\exp\{\tau'(-h_+ + (h_+^{s-1} - h_+^s)^{1/s}e^{i\pi(2l+1)/s})\} \tag{22}$$

When $h_+ > 1$, on the other hand, β_1 becomes

$$\beta_1(\tau') = \sum_{l=1}^{s} \frac{\alpha_T}{s} [1 - h_+(h_+^s - h_+^{s-1})^{-1/s}e^{-i\pi 2l/s}]$$

$$\exp\{\tau'(-h_+ + (h_+^{s-1} - h_+^s)^{1/s}e^{i\pi 2l/s})\} \tag{23}$$

For the special case of $h_+ = 1$, we find

$$\beta_1(\tau') = \alpha_T(1 - \tau')e^{-\tau'} \tag{24}$$

These solutions are shown in Fig. 8 in the transformed representation.

As seen above, $\alpha_1(\tau')$ can be expressed as a sum of exponentials, all of whose rate constants depend on s and h_+. When h_+ can be neglected compared with $|h_+^s - h_+^{s-1}|^{1/s}$,

then a Taylor expansion of $\beta_1 - \alpha_T$ shows the early time dependence to be t^s, contrary to theories involving pre-equilibrium, which predict t^2. Of course this condition is easier to achieve for smaller s, and can be seen in Fig. 8, where essentially all the $s=2$ curves start as t^2, but only the smallest h_+ curves start as t^3 or t^4 for $s=3$, 4, respectively.

Perturbative Treatment of Lower Concentrations

Of course there should be some effect of h_-, and this can be calculated perturbatively, as shown in Appendix C. Due to algebraic complexity, we only exhibit the solution valid when $\alpha_1 \approx \alpha_T$, even though the solution from Eq. 22 is valid over a wider range, provided $\alpha_1 << 1$.

Eq. 22 shows the decay of β_1 to be a sum of exponentials. Each rate constant can be written $x - h_+$, where $x = (h_+^s - h_+^{s-1})^{1/s}$. When the effects of depolymerization are included perturbatively, each rate constant acquires a correction given in Appendix C by

$$\frac{x}{s\alpha_T(h_+ - 1)(1 - h_+ + x)} - \frac{h_-}{\alpha_T}\left[1 - \frac{2}{s} - \frac{s-1}{s}\left(\frac{h_+}{x}\right)\right.$$

$$\left. - \frac{h_+}{s(1 + x - h_+)}\left(1 - \frac{x}{h_+ - 1}\right)\right]. \tag{25}$$
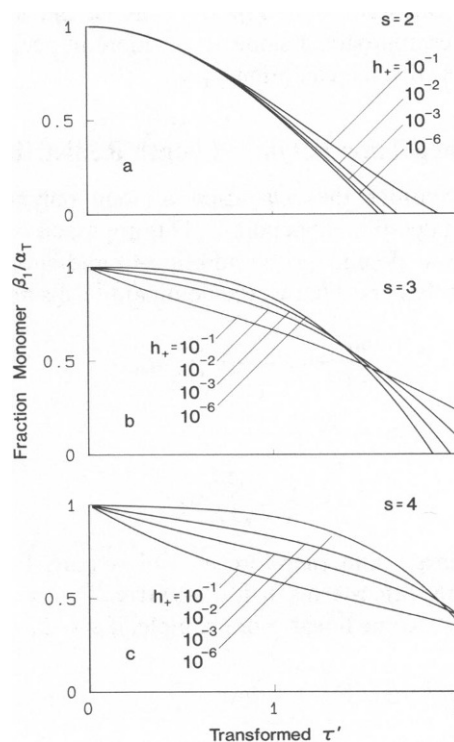

FIGURE 8 Solutions of the high-concentration limit Eqs. 22 in the τ' representation. τ' is defined in Eq. 19. For very short times, $\tau' \approx \alpha_T\tau$, but at longer times τ' and the true time variable, τ, are not so simply related. $h_+ = 10^{-6}, 10^{-4}, 10^{-3}, 10^{-2}$, as labeled. (*a*) $s = 2$ (*b*) $s = 3$ (*c*) $s = 4$. Note that for small h_+, polymerization at early times goes approximately as t^s.

These perturbative solutions can be used to define the validity conditions for the high concentration solution (when the contribution from h_- given in Eq. 25 is small) as follows. When $h_+ << 1$, the uncorrected decay time, $x - h_+$ becomes $x - h_+ \approx x \approx h_+^{(s-1)/s}$. (For purposes here, we ignore complex factors of order unity, and deal only with amplitudes.) The first term in Eq. 25 has no h_- and therefore comes from depolymerization of long polymers. For small h_+, it is always quite small compared with the unperturbed value x for $\alpha_T >> 1$, and therefore depolymerization of long polymers does not materially affect the validity of the high concentration approximation.

The second term in Eq. 25, however, comes from depolymerization of the pre-seed lengths, and to within a factor of 2 or so, it is $-h_-/\alpha_T$. The condition that it be small compared to x then becomes

$$\alpha_T >> \sigma^{-1} h_+^{1/s}. \qquad (26)$$

The point here is that simply demanding that the forward rate $h_+\alpha_1$ be much greater than the backward rate h_- would produce the condition $\alpha_T >> \sigma^{-1}$. In fact, the high concentration condition is even easier to obtain for small seed length and small h_+, due to the extra factor of $h_+^{1/s}$ in Eq. 26. This factor takes into account the fact that the flux of polymer between lengths n and $n + 1$ is biased by the relation $\alpha_n > \alpha_{n+1}$.

Note this validity condition seems to be upheld in the numerical calculations in Fig. 7. That is, the $\log \tau_D$ vs. $\log \alpha_T$ curves approach a slope of -1 more in accord with Eq. 26 than with the condition $\alpha_T >> \sigma^{-1}$.

Long Time Polymer Length Redistribution

Here we consider the relaxation of long polymers, as discussed in detail in Appendix D. Our approach is to note that $d\alpha_1/d\tau$ is dominated by addition to and subtraction from long polymers. That is, the dominant terms are

$$\frac{d\alpha_1}{d\tau} = (1 - \alpha_1) \sum_{n-s+1}^{\infty} \alpha_n.$$

When

$$\alpha_1 \approx 1, \sum_{n-s+1}^{\infty} \alpha_n$$

is usually large, and therefore α_1 will remain 1 despite changes in the other terms in $d\alpha_1/d\tau$. Given that $\alpha_1 = 1$, all other terms become linear. For example, if $s \neq 2$,

$$\frac{d\alpha_2}{d\tau} = h_+ + h_-\alpha_3 - (h_+ + h_-)\alpha_2, \qquad (27a)$$

$$\frac{d\alpha_n}{d\tau} = -(h_+ + h_-)\alpha_n + h_+\alpha_{n-1} + h_-\alpha_{n+1} \qquad n < s, \qquad (27b)$$

$$\frac{d\alpha_s}{d\tau} = -(1 + h_-)\alpha_s + h_+\alpha_{n-1} + \alpha_{n+1}, \qquad (27c)$$

$$\frac{d\alpha_n}{d\tau} = \alpha_{n-1} + \alpha_{n+1} - 2\alpha_n \qquad n > s. \qquad (27d)$$

Being linear, these equations can be solved by diagonalizing an infinite dimensional matrix. This can be done exactly for $s = 1$ and approximately when $h_+ << 1$, the usual case. The results from Appendix D show that the pre-seed lengths have a dominant relaxation rate equal to h_- as can be seen in Figs. 4–6. The post-seeds have an infinite set of relaxation rates, λ, that fall in the range $-4 < \lambda < 0$. The eigenvector associated with a given λ (i.e. the configuration of long polymers that relaxes at rate λ) is given by $\sin [n \cos^{-1}((\lambda + 2)/2)]$. In other words, a relaxation rate of λ corresponds to a "spatial" (in the concentration vs. length space) frequency of $\cos^{-1}([\lambda + 2]/2)$. Thus for long spatial periods, P, the relaxation times are $T = (P/2\pi)^2$. This result is essentially that for diffusion, since any one polymer may be envisioned as taking a random walk in length space. Thus changes in length by amount P require amounts of time that scale as P^2.

If we set P equal to the average polymer length in equilibrium, then we find the "typical" relaxation time for the long polymers is $\alpha_T/4\pi^2\omega$. (Remember, of course, that the relaxation of a particular length takes place over many times λ^{-1}.) To make this concrete, if $g_- = 1$ s^{-1} and $\omega = 10^{-6}$, polymer relaxation may well take weeks, even though monomer relaxation may take only minutes.

Long Seed: Establishment of Pre-equilibrium

When the seed size is large and α_T small, the effect of long polymers on the monomer kinetics takes a very long time. In the meanwhile, the pre-seeds may have time to equilibrate with the initial monomer concentration. This situation is mathematically identical with the $s = 1$ condition, at least up to the time when the long polymers accumulate. Thus by examining the $s = 1$ case, we can derive the time needed for the pre-seeds to reach pre-equilibrium. If this time is less than the monomer decay time, then the usual pre-equilibrium assumption is valid.

The details of the $s = 1$ polymerization are given in Appendix E. The relaxation time for polymers of length n to equilibrate with the monomer, provided that $\alpha_T\sigma << 1$, is

$$(-1 - \alpha_T\sigma + 2\sqrt{\alpha_T\sigma})^{-1} h^{-1} [1 + \ln (n - 1)]. \qquad (28)$$

This time must be substantially less than the time for monomer relaxation if the pre-equilibrium assumption is to hold. A lower bound on the monomer decay time can be obtained from the high concentration limit, even though the reaction is not at high concentration. The true relaxation time may be much slower, so the following condition is somewhat conservative. Nevertheless, we can calculate the $1/e$ delay time for monomer decay from Appendix B. The resulting condition for the validity of the pre-equilibrium

assumption is

$$\alpha_T \sigma [1 + \ln(s-1)](h_+/s!)^{1/s} << 1 + \alpha_T \sigma - 2\sqrt{\alpha_T \sigma}. \quad (29)$$

It would seem that this condition is easy to satisfy, but it must be remembered it is derived assuming $\alpha_T << \sigma^{-1}$, $s >> 1$, and $h_+ << 1$. In fact, there is no pre-equilibrium when $s = 4$ and $\alpha_T \approx \sigma$, (calculation not shown) but Fig. 6 shows an excellent pre-equilibrium when $s = 10$ and $\alpha_T \approx \sigma$.

PREVIOUS INVESTIGATIONS

Oosawa (1, 15) and collaborators pioneered work on protein polymerization. They drew the analogy with condensation phenomena, pointed out the importance of the critical concentration, and showed that the time scale for monomer decay was very different from the time scale for polymer length redistribution. Oosawa also used the pre-equilibrium assumption in deriving kinetic solutions, including the result that d $\log \tau_D$/d $\log \alpha_\tau = -s/2$. This assumption and result have since been used by many workers (10) for data analysis. But as Frieden and Goddette (11) have shown numerically and we have shown analytically, the pre-equilibrium assumption is highly suspect, particularly for small seeds. Why was this not discovered earlier?

The pre-equilibrium hypothesis is attractive because it reduces an infinite set of equations to two, and advanced at a time when large computers were not as powerful or as accessible as today. Further, there was no direct experimental way to check the simple theory. Particularly since it is believed that many protein polymerization reactions are more complicated than the basic model discussed here, one could always ascribe discrepancies to ATP hydrolysis, fragmentation reactions, conformational changes, etc. It gave sensible sigmoidal polymerization curves, and the fact that too many polymers were predicted was attributed (somewhat justifiably) to the assumption of irreversibility.

Wegner and Engel (3) used a steady state assumption (i.e. $d\alpha_2/d\tau \approx 0$) to derive an equation similar (but by no means identical) to the pre-equilibrium Eq. 11. Their mathematics corresponds to our definition of $s=2$, although they used a different definition of seed size. As it turns out, this steady state assumption is nearly true when $s=2$ and $\tau \approx 0$. Wegener and Engel tested their equations against computer solutions of the exact equations for two similar conditions ($\alpha_T = 3.74$ in both cases, $\sigma = 6 \times 10^{-7}$ in one case and $\sigma = 2.2 \times 10^{-7}$ in the other) and found the results quite acceptable with regard to monomer relaxation. This success was later taken (4, 10) as justification for applying the pre-equilibrium assumption to all seed lengths.

In many cases a pre-seed is more likely to decay than to elongate ($h_- >> h_+ \alpha_1$, or $\alpha_1 << \sigma^{-1}$, almost the antithesis of the high concentration limit used here). Thus many cycles of elongation/decay must occur before the pre-seed

becomes a seed, and there is plenty of time for pre-equilibrium to occur. Although it is often true that $\alpha_T < \sigma^{-1}$, the curves in Fig. 7 seem to be in the high concentraton limit (i.e. show no effects of h_-) even when α_T is several orders of magnitude less than σ^{-1}. Why does the validity condition for high concentration, Eq. 26, have the apparent extra factor of $h_+^{1/s}$?

One answer is as follows: Instead of comparing the rates of decay and elongation for a given pre-seed, consider the "flux" of concentration between two adjacent pre-seed sizes, for example n and $n+1$. Thus we compare the elongation rate of the nth-mer, $h_+ \alpha_n \alpha_1$ and the depolymerization rate of the $n+1^{th}$-mer, $h_- \alpha_{n+1}$. The net flux must be toward the longer oligomers because we are studying a (net) polymerization reaction, and the flux is positive mainly because $\alpha_n >> \alpha_{n+1}$, not simply because $\alpha_1 > \sigma^{-1}$. In other words, we are justified in ignoring the depolymerization step for length n (in some circumstances), not because it is small compared with the elongation rate of size n, but because it is small compared with the elongation reaction of size $n-1$.

This reasoning works provided $\alpha_n >> \alpha_{n+1}$ where both n and $n+1$ are pre-seed sizes. The ratio α_n/α_{n+1} is actually accentuated as n gets closer to s, due to mass action as can be seen in the "plateau" region of Fig. 6). Thus if the seed size is very large, we expect the early pre-seed lengths to be more nearly equal, and the high concentration limit harder to achieve. On the other hand, if the seed length is small, all the pre-seeds are affected by the seed, and the high concentration limit (or at least its perturbative expansion) is applicable over a wider range of α_T than simply $\alpha_T >> \sigma^{-1}$. This is exactly the effect of the "extra" factor $h_+^{1/s}$ in Eq. 26. We conclude that small seed reactions can, and in some cases should, be treated differently than large seed reactions.

EXPERIMENTAL DETERMINATION OF KINETIC PARAMETERS

We outline in this section a way of determining the various kinetic parameters from experimental data, based on the above solutions. We emphasize that this method may not be optimal—a better method might be based on lower concentration experiments, but the theory is harder to deal with in that region. Note, however, that the theory is simpler in the high concentration region, and particularly that there are fewer parameters. Thus fitting to both low and high concentration ranges may give a much better test of the applicability of the original Eqs. 2 than fitting to either concentration range alone. It is always possible, of course, to resort to numerical fitting of the (numerical) solutions of Eqs. 2, but this may in some cases take an impractical length of time.

A detailed discussion of the practicalities of making measurements would be out of place here. We shall assume in the following that some measure of the monomer

concentration as a function of time is available, possibly from fluorescence, light scattering, viscosity, chemical separation, microscopy, or other methods. We emphasize that any technique allowing the measurement of concentrations of specific lengths other than monomer (e.g. in some cases, electron microscopy) is an extremely valuable addition to techniques that simply measure the monomer alone. It would allow the separation of many theoretical possibilities that would otherwise appear similar on the basis of monomer disappearance over a limited (by perhaps practical aspects) concentration range.

First we note that the critical concentration (equal to g_-/g_+) can be obtained from equilibrium measurements. g_+ can be obtained by adding monomer to a known number of long filaments and recording the initial rate of polymerization (16).

With g_+ and g_- in hand, the polymerization experiment starting with only monomer should be run at high enough concentration such that $d \log t_D/d \log \alpha_T = -1$. From the absolute value of t_D at these concentrations, one can numerically determine a relation between seed size and h_+. That is, numerical solutions of Eqs. 18 can be used to generate $\log t_D$ vs. $\log \alpha_T$ curves for a given seed size, as in Fig. 7. The results will be independent of h_- for large enough α_T, and the absolute time scale will depend only on h_+ and s. Actually, if the delay time is picked so that $\alpha_1 \approx \alpha_T$, then Eq. 22 can be used instead of the more laborious process of solving Eqs. 18.

Once h_+ is known for a given seed size, h_- can be determined from the slope of t_D at smaller values of α_T where $\log t_D$ vs. $\log \alpha_T \neq -1$, again for a given seed size.

At this point each tentative seed size has an associated h_+ and h_-, and the experimental curves can be directly compared with simulated curves, one curve per seed size. This comparison is definitely diagnostic of seed size when α_T is large and $h_+^{1/s} \ll 1$, as noted above, and probably diagnostic at other values as well. Once the seed size is determined, the experimental curves should be compared with the theoretical ones for a wide variety of α_T values, as a validation procedure. If this procedure shows discrepancies, then the original model, Eqs. 2, may not be appropriate.

PROSPECTS

We have presented extensive analysis of the simplest cooperative polymerization scheme, and an experimental strategy to determine the relevant parameters. But what if the experimental reaction does not have this simple form? Our experimental procedure can probably establish that certain data are consistent with the simple model, but it does not establish uniqueness. Further, there may be other complicating factors. For example, actin polymerization in vivo involves an ATP-ADP cycle (5, 6, 17). Consequently, the rate constants are different for the two polymer ends. Furthermore, fragmentation and reannealing may occur. We briefly address these issues below.

First, polymerization reactions may differ simply by changes in scale, represented by g_- and g_+, and not in the internal physics, represented by s, h_+, and σ. It is conceivable, for example, that the effect of ATP hydrolysis on actin polymerization is simply a change of scale—ADP-actin does polymerize, albeit with a higher critical concentration, and it has been suggested that the ATP hydrolysis takes place on the inner monomer units, not on the ends of the polymer. One could thus imagine that under high concentration conditions, the binding of ATP to monomeric actin would shift the time and concentration scales relative to ADP-bound actin, but leave everything else the same. This possibility must be checked at high concentration, since otherwise there is the complication of polymerizing with an ATP-monomer but depolymerizing with an ADP-end unit, a complication that affects the statistics (and perhaps the biology), but not the underlying physics. Of course, the ATP hydrolysis may well affect h_+ and σ, as well as increase the complexity of the reaction by requiring two types of monomer and many types of polymer (depending on the statistical arrangement of ATP and ADP along the chain).

One simple extension to our model is to assume the rate constants depend on polymer length up to some length, s. This increases the number of parameters to fit, but does not affect our basic formalism, and in particular does not affect our conclusions based on scaling arguments, nor the simplification obtained at high concentration. Frieden and Goddette (11) use this extension in their numerical simulations of actin polymerization, and have also concluded that the pre-equilibrium assumption is often suspect.

Potentially more troublesome are the possibilities of fragmentation, reannealing, and/or heterogeneous seed formation. These processes will not affect the thermodynamics of polymerizaton (in contrast to ATP hydrolysis), but will affect reaction rates via terms in the differential equations that have not been considered here. Thus our scaling arguments may be affected in a model-dependent way. One possible approach is that of Bishop and Ferrone (12) who use a perturbative expansion near $\tau = 0$, and show that these "extra" processes can often be represented by addition of simple terms in a general way. The solutions of their equations then provides diagnostics for which processes are actually involved experimentally. However, Bishop and Ferrone made the pre-equilibrium assumption, which cannot be relied upon for small seed lengths or at high concentration. Still, their conclusions may be warranted for large seeds and low concentrations, as for sickle-cell hemoglobin (18), and their approach of classifying cooperative polymerization processes by the type of differential equation involved may prove useful even when the pre-equilibrium assumption is not valid. We note that in a slightly different context, fragmentation and reannealing play a major role in colloid formation. See, for example, Heicklen (7), Bentz and Nir (8), Hendriks and Ernst (9) and references contained therein.

SUPPLEMENTAL MATERIAL

Upon request, the authors will furnish the results of five more sample calculations, similar to Figs. 4 and 5, but for different values of α_T, h_+, or h_-.

APPENDIX A

We derive here the total number of polymers in equilibrium, $C(\tau \to \infty)$, for the pre-equilibrium/irreversible assumptions. The equations to be solved are:

$$\frac{d\alpha_1}{d\tau} = C - C\alpha_1 \tag{A1}$$

$$\frac{dC}{d\tau} = K\alpha_1^{s-1}(\alpha_1 - 1). \tag{A2}$$

Note that by simply setting the derivatives to zero, we find that $\alpha_1(\infty) \to 1$ but that $C(\infty)$ is not determined.

Define $z = \ln(\alpha - 1)$, and therefore

$$\frac{dz}{d\tau} = \frac{1}{\alpha_1 - 1}\frac{d\alpha_1}{d\tau} = -C, \tag{A3}$$

Thus

$$\frac{d^2z}{d\tau^2} = -\frac{dC}{d\tau} = -K\alpha_1^{s-1}(\alpha_1 - 1). \tag{A4}$$

But

$$\frac{d^2z}{d\tau^2} = \frac{dz}{d\tau}\frac{d}{dz}\frac{dz}{d\tau},$$

and since at $\tau = 0$, $dz/d\tau = -C = 0$, then

$$\int_0^{C(\infty)} \frac{dz}{d\tau} d\left\{\frac{dz}{d\tau}\right\} = -K\int_{\alpha_T}^{\alpha_1(\infty)} \alpha_1^{s-1} d\alpha_1. \tag{A5}$$

Since $\alpha_1(\tau \to \infty) = 1$,

$$C(\infty) = \left[\frac{2K}{s}(\alpha_T^s - 1)\right]^{1/2}. \tag{A6}$$

APPENDIX B

Here we solve the high-concentration limit of the exact kinetic equations. Note that every quadratic polymerization term in Eqs. 3 contains an α_1 factor. If time can be transformed in such a way that the right-hand side can be divided by $\alpha_1(\tau)$, then we will have achieved the necessary transformation. Thus we set

$$\tau' = \int_0^\tau \alpha_1(t_0)dt_0 \tag{B1}$$

and note that

$$\frac{d}{d\tau} = \frac{d\tau'}{d\tau}\frac{d}{d\tau'} = \alpha_1\frac{d}{d\tau'}. \tag{B2}$$

We shall use the notation that

$$\beta_n(\tau') = \alpha_n(\tau); \quad G(\tau') = C(\tau), \tag{B3}$$

because even though $\beta_n(\tau')$ and $\alpha_n(\tau)$ refer to the concentration of the nth polymer, they are different functions of their respective arguments. Eq. B1 is the requisite transformation, and once $\beta_1(\tau)$ is found, the inverse transformation can be calculated from

$$\tau = \int_0^{\tau'} \frac{dt_0}{\beta_1(t_0)}. \tag{B4}$$

Thus in the absence of depolymerization, the kinetic equations become

$$\frac{d\beta_1}{d\tau'} = -2h_+\beta_1 - h_+\sum_{n=2}^{s-1}\beta_n - G - \beta_s \tag{B5a}$$

$$\frac{d\beta_n}{d\tau'} = h_+(\beta_{n-1} - \beta_n) \quad 2 \le n < s \tag{B5b}$$

$$\frac{d\beta_s}{d\tau'} = h_+\beta_{s-1} - \beta_s \tag{B5c}$$

$$\frac{dG}{d\tau'} = \beta_s. \tag{B5d}$$

We now have a set of $s+1$ linear first-order differential equations. One way to solve them is to take the derivative of both sides of Eq. B5a, and by substituting from Eqs. B5b–d, we obtain

$$\left(\frac{d}{d\tau'} + h_+\right)^2\beta_1 = (h_+^2 - h_+)\beta_{s-1}. \tag{B6}$$

Note that Eq. B5b is equivalent to

$$\left(\frac{d}{d\tau'} + h_+\right)\beta_n = h_+\beta_{n-1} \quad 2 \le n < s, \tag{B7}$$

and therefore we can reduce Eq. B6 to

$$\left(\frac{d}{d\tau'} + h_+\right)^s\beta_1 = (h_+^s - h_+^{s-1})\beta_1. \tag{B8}$$

This has the solution $\beta_1 = \exp\{R\tau'\}$, where R is given by

$$R = -h_+ + (h_+^s - h_+^{s-1})^{1/s}. \tag{B9}$$

When $h_+ \ne 1$, there are s independent solutions for R, and β_1 is simply a sum of exponentials. If $h_+ = 1$, on the other hand, R is real and degenerate, and β_1 is an s-order polynomial in τ' times an exponential. In either case, the coefficients are determined by initial conditions—the derivatives of β_1 at $\tau' = 0$—as follows: From Eqs. B6 and B7,

$$\left[\left(\frac{d}{d\tau'} + h_+\right)^n\beta_1\right]_{\tau'=0} = 0 \quad \text{for} \quad 2 \le n < s. \tag{B10}$$

Thus $\beta_1(0) = \alpha_T$ and $d\beta_1(0)/d\tau' = 2h_+\alpha_T$ and by induction,

$$\left(\frac{d}{d\tau'}\right)^n\beta_1(0) = (n+1)(-h_+)^n\alpha_T \quad n < s, \tag{B11}$$

and from Eq. B8, we also find

$$\left(\frac{d}{d\tau'}\right)^s \beta_1(0) = \alpha_T[h_+^s - h_+^{s-1} - (s+1)(-h_+)^s]. \quad (B12)$$

When $h_+ \neq 1$, the solution for $\beta_1(\tau')$ can be written

$$\beta_1(\tau') = \sum_{n=1}^{s} B_n \exp\{\tau'(-h_+ + y e^{2n i \pi/s})\}, \quad (B13)$$

where

$$y = |h_+^s - h_+^{s-1}|^{1/s} \qquad h_+ > 1 \quad (B13a)$$

$$y = e^{i\pi/s}|h_+^s - h_+^{s-1}|^{1/s} \qquad h_+ < 1 \quad (B13b)$$

By considering the nth derivative of $e h_+ \tau' \beta_1$ at $\tau' = 0$, then Eqs. B11-B13 imply that

$$\sum_{n=1}^{s} B_n = a_T \quad (B14)$$

$$\sum_{n=1}^{s} B_n e^{i\pi(2n+1)/s} = -\alpha_T h_+ (h_+^{s-1} - h_+^s)^{-1/s} \quad (B15)$$

$$\sum_{n=1}^{s} B_n e^{i\pi m(2n+1)/s} = 0 \qquad 2 \leq m < s. \quad (B16)$$

These equations for B_n can be solved by a discrete Fourier transform, and the result for β_1 is

$$\beta_1(\tau') = \sum_{n=1}^{s} \frac{\alpha_T}{s}\left[1 - \frac{h_+}{y} e^{-2n i \pi/s}\right]$$

$$\cdot \exp\{\tau'(-h_+ + y e^{2n i \pi/s})\}. \quad (B17)$$

When $h_+ = 1$, (no kinetic cooperativity), then β_1 has the special solution

$$\beta_1(\tau') = \alpha_T(1 - \tau')e^{-\tau'}. \quad (B18)$$

These solutions (Eqs. B17) are shown in Fig. 8 for various values of s and h_+, in the τ' representation. Remember, from Eq. B4, that $\beta_1(\tau') = 0$ corresponds to $\tau = \infty$.

When $h_+^{1/s} \ll 1$, β_1 can be easily expanded in a Taylor series about $\tau' = 0$. Since the coefficient of the $(\tau^k/k!)$ term in the Taylor expansion is simply the kth derivative of β_1 evaluated at $\tau' = 0$, then

$$\left(\frac{d}{d\tau'}\right)^k \beta_1(0) = \sum_{n=1}^{s} \frac{\alpha_T}{s}\left[1 - \frac{h_+}{y} e^{-2in\pi/s}\right][-h_+ + y e^{2in\pi/s}]^k \quad (B19)$$

and in the limit that $h_+ \ll y$, i.e. $h_+^{1/s} \ll 1$,

$$\left(\frac{d}{d\tau'}\right)^k \beta_1(0) = \frac{\alpha_T}{s} y^k \sum_{n=1}^{s} e^{2ni\pi k/s} = -\alpha_T \quad \text{for} \quad k = s$$

$$= 0 \qquad \text{for} \quad k < s. \quad (B20)$$

Thus $\beta_1 \approx \alpha_T(1 - h_+^{s-1} - (\tau')^s/s! + \cdots)$. This special form is clearly diagnostic of the seed size, but is not valid for all values of h_+. It is in general not possible to transform back to the τ representation exactly. For very short times, when $\beta_1 \approx \alpha_T$, of course $\tau' = \tau\alpha_T$, and for slightly longer times, a Taylor expansion could be used. Extensive numerical approximations to transform back to τ probably involve more work than simply solving Eqs. 18 numerically, but the analytical solutions in τ' are themselves useful at small τ' and also as test cases for diagnostic analysis of various parameters. If a certain procedure for determining the seed, for example, doesn't work in the τ' representation, then it is unlikely to work in the τ representation, at least in the high concentration limit.

APPENDIX C

Yet another way to solve Eqs. B5 is by matrix methods, which will prove more useful with the perturbation theory to follow. We define $\beta_0 = d\beta_0/d\tau'$ and $\beta^\dagger = (\beta_0, \beta_1, \cdots \beta_s)$, and then write Eqs. B5 as

$$\frac{d\beta}{d\tau'} = M \cdot \beta, \quad (C1)$$

where M is given by

$$M = \begin{bmatrix} -2h_+ & -h_+^2 & 0 & 0 & 0 & \ldots & 0 & h_+^2 - h_+ & 0 \\ 1 & 0 & 0 & 0 & 0 & \ldots & 0 & 0 & 0 \\ 0 & h_+ & -h_+ & 0 & 0 & \ldots & 0 & 0 & 0 \\ 0 & 0 & h_+ & -h_+ & 0 & \ldots & 0 & 0 & 0 \\ \ldots & \ldots & \ldots & \ldots & \ldots & \ldots & \ldots & \ldots & \ldots \\ 0 & 0 & 0 & 0 & 0 & \ldots & h_+ & -h_+ & 0 \\ 0 & 0 & 0 & 0 & 0 & \ldots & 0 & h_+ & -1 \end{bmatrix}.$$

$$(C2)$$

The eigenvalues and eigenvectors can be found and the solutions below can be verified by substitution. Note that since M is not Hermitian, we need to calculate both the right and left eigenvectors, which are not equal in general. The eigenvalues λ are given by $\lambda = -1$ and $\lambda = -h_+ + (h_+^s - h_+^{s-1})^{1/s}$. For notational convenience, let $x = (h_+^s - h_+^{s-1})^{1/s}$, and if the right (left) eigenvectors are designated R(L), then for $\lambda = -1$ we find

$$L = \begin{bmatrix} h_+/(h_+ - 1)^2 \\ h_+(2h_+ - 1)/(h_+ - 1)^2 \\ 1 \\ (h_+ - 1)/h_+ \\ [(h_+ - 1)/h_+]^2 \\ \cdots \\ [(h_+ - 1)/h_+]^{s-3} \\ \frac{h_+}{1 - h_+} + \left(\frac{h_+ - 1}{h_+}\right)^{s-2} \end{bmatrix} \qquad R = \begin{bmatrix} 0 \\ 0 \\ \cdots \\ 0 \\ 1 \end{bmatrix} \quad (C3)$$

and for $\lambda = -h_+ + x$,

$$L = \begin{bmatrix} (x/h_+)^{s-2}/(h_+ - 1) \\ (x/h_+)^{s-2}(x + h_+)/(h_+ - 1) \\ 1 \\ x/h_+ \\ (x/h_+)^2 \\ \cdots \\ (x/h_+)^{s-3} \\ 0 \end{bmatrix}$$

$$R = \begin{bmatrix} x - h_+ \\ 1 \\ h_+/x \\ (h_+/x)^2 \\ \cdots \\ (h_+/x)^{s-2} \\ (h_+/x)^{s-2}h_+/(1 + x - h_+) \end{bmatrix} \quad (C4)$$

These eigenvectors can be used in perturbation theory in the following way. To find the eigenvalues and eigenvectors of $M + \Lambda M'$, where Λ is a small parameter, expand the right eigenvector as

$$R = \sum_{n=0}^{\infty} \Lambda^n R^{(n)},$$

similarly for the left eigenvector, and expand the eigenvalue as

$$\lambda = \sum_{n=0}^{\infty} \Lambda^n \lambda^{(n)}.$$

Then substitute into $(M + \Lambda M')R = \lambda R$, and solve by powers of Λ. For Λ^0, we get

$$M \cdot R^{(0)} = R^{(0)} \quad (C5)$$

and for Λ^1 we find

$$M \cdot R^{(1)} + M' \cdot R^{(0)} = \lambda^{(1)}R^{(0)} + \lambda^{(0)}R^{(1)}. \quad (C6)$$

Multiply Eq. C6 on the left by the zero-order left eigenvector $L^{(0)}$ and solve for $\lambda^{(1)}$ to obtain

$$\lambda^{(1)} = \frac{L^{(0)} \cdot M' \cdot R^{(0)}}{L^{(0)} \cdot R^{(0)}}. \quad (C7)$$

Thus the first-order correction to the eigenvalues may be obtained by using $L^{(0)}$ and $R^{(0)}$ from Eq. C4 and by deriving M' from the basic differential equations. Even though Eqs. C1–C2 are valid over a wide range of β_1, we shall now derive M' by assuming $\beta_1 \approx \alpha_T$; that is, our use of M' will be limited to the initial phase of monomer relaxation. This greatly facilitates the mathematics, and is still useful for determining $d (\log \tau_D)/d (\log \alpha_T)$ provided the polymerization reaction not gone too far.

We now keep all terms during the transformation of Eqs. 18 into Eqs. B5, and then discard all terms quadratic or higher in $1/\beta_1$. In other words, we allow depolymerization reactions to occur before the seed (perturbatively), but still forbid depolymerization of the seed-plus-one length. We also assume that the small parameter, $\Lambda = 1/\beta_1 \approx 1/\alpha_T$, which limits the validity of this approximation to early times. In this way, M remains as in Eq. C2, and M' becomes

$$M = \begin{bmatrix} 0 & 2h_+h_- & 0 & 0 & 0 & 0 & \cdots & 0 & 1 - h_+h_- \\ 0 & 0 & 0 & 0 & 0 & 0 & \cdots & 0 & 0 \\ 0 & 0 & -h_- & h_- & 0 & 0 & \cdots & 0 & 0 \\ 0 & 0 & 0 & -h_- & h_- & 0 & \cdots & 0 & 0 \\ \cdots & \cdots & \cdots & \cdots & \cdots & \cdots & \cdots & \cdots & \cdots \\ 0 & 0 & 0 & 0 & 0 & 0 & \cdots & -h_- & h_- \\ 0 & 0 & 0 & 0 & 0 & 0 & \cdots & 0 & -h_- \end{bmatrix}$$

$$(C8)$$

By applying Eq. C7, we find that the first-order correction to the eigenvalue $\lambda^{(0)} = -1$ is

$$\lambda^{(1)} = (1 - h_+)^{-1}\left[1 - \left(\frac{h_+ - 1}{h_+}\right)^{s-1}\right]^{-1} - \frac{h_-}{1 - h_+}, \quad (C9)$$

and the correction to the eigenvalues $\lambda^{(0)} = -h_+ + x$ are

$$\lambda^{(1)} = \frac{x}{s(h_+ - 1)(1 + x - h_+)} - h_-\left(1 - \frac{2}{s}\right)$$
$$+ h_- \cdot \left[\frac{s - 1}{s}\left(\frac{h_+}{x}\right) + \frac{h_+}{s(1 + x - h_+)}\left(1 - \frac{x}{h_+ - 1}\right)\right]. \quad (C10)$$

APPENDIX D

Once the polymerization reaction reaches the $\alpha_1 = 1$ stage, the resulting differential equations are linear, and are amenable to matrix manipulations. In contrast with the earlier appendices, the matrices used here are infinite dimensional, and require somewhat different techniques.

An infinite-dimensional matrix has an infinite number of eigenvalues; the number of eigenvalues may be countable or uncountable, and the eigenvalue spectrum may be discrete or continuous. As an example, consider the quantum mechanical simple harmonic oscillator. Both the Hamiltonian and the momentum operator can be written in matrix form with a countable number of rows and columns, using the energy eigenvector representation. The eigenvalue spectrum of the Hamiltonian is discrete, countable, and bounded from below, while the corresponding spectrum of the momentum matrix is continuous, uncountable, and unbounded. In the particular case for this appendix, we will solve the matrix eigenvalue equation by transforming it into a differential equation for a generating function, and then show that the eigenvalues form a continuous spectrum, bounded on both sides.

If we define $\alpha^\dagger = (\alpha_2, \alpha_3, \cdots)$, then the differential equation can be written

$$\frac{d\alpha}{d\tau} = R\alpha + (h_+, 0, 0, \ldots)^\dagger. \quad (D1)$$

If, for example, $s = 4$, R is given by

$$R = \begin{bmatrix} -h_+ - h_- & h_- & 0 & 0 & 0 & 0 & \ldots \\ h_+ & -h_+ - h_- & h_- & 0 & 0 & 0 & \ldots \\ 0 & h_+ & -h_+ - h_- & 1 & 0 & 0 & \ldots \\ 0 & 0 & 1 & -2 & 1 & 0 & \ldots \\ 0 & 0 & 0 & 1 & -2 & 1 & \ldots \\ \ldots & \ldots & \ldots & \ldots & \ldots & \ldots & \ldots \end{bmatrix}.$$

(D2)

Note that R is tridiagonal and that $\text{sign}(R_{ij}) = \text{sign}(R_{ji})$. Such a matrix is guaranteed to have real (and in our case negative) eigenvalues, and can be cast into symmetric form (19) by a similarity transformation that effectively replaces R_{ij} with $(R_{ij}R_{ji})^{1/2}$. If this is done, and we note that usually $h_+ << h_-$, i.e. the reaction is highly cooperative, then the pre-seed entries along the main diagonal (in Eq. D2 the first and second entries corresponding to the dimer and trimer) become nearly block diagonal. This means the pre-seeds have a dominant relaxation rate of $h_- + h_+$, as evidenced in Figs. 4–6.

Once the pre-seed relaxations have been solved as nearly block-diagonal, the remaining task is to solve for the eigenvalues of $R' = S - 2I + R'_P$, where I is the unit matrix, and

$$S = \begin{bmatrix} 0 & 1 & 0 & 0 & 0 & \ldots \\ 1 & 0 & 1 & 0 & 0 & \ldots \\ 0 & 1 & 0 & 1 & 0 & \ldots \\ \ldots & \ldots & \ldots & \ldots & \ldots & \ldots \end{bmatrix},$$

(D3)

$$R'_P = \begin{bmatrix} 2 - h_+ - h_- & 0 & \ldots \\ 0 & 0 & \ldots \\ \ldots & \ldots & \ldots \end{bmatrix}.$$

(D4)

R' been decomposed in this manner to draw a mathematical analogy with the problem of phonon structure in one-dimensional crystals. S then represents a semi-infinite chain of atoms with identical nearest-neighbor interactions, while R'_P represents a substitutional impurity at the end position. $-2I$ simply shifts all eigenvalues equally, and can be added back at the end of the calculation. The physics of impurity vibrations shows that the effect of R'_P is to significantly shift at most one eigenvalue (20), and that because our case corresponds to lighter-than-normal atom substitution, the resulting shifted eigenvalue corresponds to a localized vibration outside the normal spectrum. In our terms, this means the seed length (impurity atom) acquires a somewhat faster relaxation rate, but this extra rate has little effect on the other lengths.

It remains to find the eigenvalues and eigenvectors of S. Let $\mathbf{v}$ be an eigenvector of S with eigenvalue Λ. From the definition of S, then

$$\mathbf{v}_2 = \Lambda v_1$$

(D5)

$$v_{n-1} + v_{n+1} = \Lambda v_n$$

(D6)

Eq. D6 is exactly the recursion relation for Chebyshev polynomials, and indeed, they are closely related to the final eigenvectors. If we multiply Eq. D6 by $x^n/n!$, then sum from $n = 2$ to ∞, and then add x times Eq. D5,

we obtain

$$\sum_{n=2}^{\infty} \frac{x^n v_{n-1}}{n!} + \sum_{n=1}^{\infty} \frac{x^n v_{n+1}}{n!} = \sum_{n=1}^{\infty} \frac{x^n v_n}{n!}.$$

(D7)

If we shift dummy variable, n, on the first two sums and then take the derivative of the entire equation, the result can be written

$$\frac{d^2 f(x)}{dx^2} - \Lambda \frac{df(x)}{dx} + f(x) = 0,$$

(D8)

where

$$f(x) = \sum_{n=1}^{\infty} \frac{x^n v_n}{n!}.$$

Thus we can solve Eq. D8 for $f(x)$ and then obtain v_n from

$$v_n = \left[\left(\frac{d}{dx} \right)^n f(x) \right]_{x=0}$$

(D9)

The solution of Eq. D8 takes the form $f(x) = e^{kx}$, where k is given by $k = (\Lambda/2) \pm [(\Lambda/2)^2 - 1]^{1/2}$. If $|\Lambda| > 2$, the corresponding v_n grow without limit, and we must reject these solutions as incompatible with conservation of total protein. If $|\Lambda| < 2$, on the other hand, v_n is bounded. In particular, from Eq. D9,

$$v_n = \sin [n \cos^{-1}(\Lambda/2)].$$

(D10)

Thus the eigenvalues λ of $S - 2I$ become $\lambda = \Lambda - 2$, and for each eigenvalue $-4 < \lambda < 0$, the eigenvector is given by $v_n^{(\lambda)} = \sin[n\cos^{-1}(\lambda + 2)/2]$.

APPENDIX E

Here we estimate the time required for a given polymer length to come to equilibrium for a seed of one and $\alpha_T << \sigma^{-1}$. This is a useful analogy to the situation when the seed length is very long, and can be used to a lower bound for the time necessary to achieve pre-equilibrium of pre-seeds. Since $s = 1$, we set $h_+ = h_- = 1$ with no loss of generality. The fractional change in α_1 from $\tau = 1$ to $\tau = \infty$ is given by

$$\frac{\alpha_T - \alpha_1(\infty)}{\alpha_T} = \frac{\alpha_T}{1 + \alpha_T}$$

(E1)

from the true equilibrium Eqs. 4, and therefore when $\alpha_T << 1$, we are justified in assuming $\alpha_1 = \alpha_T$ throughout the reaction. The differential equations become linear in this regime,

$$\frac{d\alpha_2}{d\tau} = \alpha_T(\alpha_T - \alpha_2) + \alpha_3 - \alpha_2$$

(E2)

$$\frac{d\alpha_n}{d\tau} = \alpha_T(\alpha_{n-1} - \alpha_n) + \alpha_{n+1} - \alpha_n \quad n > 2.$$

(E3)

This can be written symbolically as

$$\frac{d\alpha}{d\tau} = M\alpha + \mathbf{b},$$

(E4)

where $\alpha^t = (\alpha_2, \alpha_3, \cdots)$ and the solution

$$\alpha(\tau) = (e^{M\tau} - I)M^{-1}\mathbf{b}.$$

(E5)

$M^{-1}\mathbf{b}$ gives the equilibrium solution,

$$(M^{-1}\mathbf{b})^T = (-\alpha_T^2, -\alpha_T^3, \ldots),$$

(E6)

and $\exp\{M\tau\}$ can be found as follows. Define the diagonal matrix C as $C_{ij} = \delta_{ij}\alpha_T^{1-i}$, and then note that

$$CMC^{-1} + (\alpha_T + 1)I = \sqrt{\alpha_T} \begin{bmatrix} 0 & 1 & 0 & 0 & \cdots \\ 1 & 0 & 1 & 0 & \cdots \\ 0 & 1 & 0 & 1 & \cdots \\ 0 & 0 & 1 & 0 & \cdots \\ \cdots & \cdots & \cdots & \cdots & \cdots \end{bmatrix}. \qquad (E7)$$

This is exactly the same matrix dealt with in Appendix D. Thus the eigenvalues of M are $-1-\alpha_T+\Lambda\sqrt{\alpha_T}$ where $-2<\Lambda<2$. We use the fact that the eigenvectors are given by $\sin(n\cos^{-1}[\Lambda/2])$ to (a) transform M to diagonal form, (b) exponentiate, and (c) transform back to the original representation. Thus

$$(e^{M\tau})_{jk} = \int_{-2}^{2} d\Lambda F(\Lambda) \sin\left(j\cos^{-1}\frac{\Lambda}{2}\right) e^{\tau(-1-\alpha_T+\Lambda\sqrt{\alpha_T})}$$
$$\cdot \sin\left(k\cos^{-1}\frac{\Lambda}{2}\right)\alpha_T^{j-k}, \quad (E8)$$

where $F(\Lambda)$ contains any normalization of the eigenvectors. The result is

$$\frac{\alpha_j(\tau)}{\alpha_T^j} = 1 - \int_{-2}^{2} d\Lambda F(\Lambda) \sin\left([j-1]\cos^{-1}\frac{\Lambda}{2}\right) e^{\tau(-1-\alpha_T+\Lambda\sqrt{\alpha_T})}$$
$$\cdot \sum_{k=1}^{\infty} \sin\left(k\cos^{-1}\frac{\Lambda}{2}\right). \quad (E9)$$

Note that the time for a term such as Ae^{-kt} to decay to e^{-1} is $t = [\ln(A)+1]/k$. If we assume the integral in Eq. E9 is dominated by the slowest decay time (thus producing an upper bound on the decay time), then $\Lambda \approx 1$. After putting back the constants h_+ and h_-, the decay time to equilibrium for the nth species, $\tau_{D,n}$ becomes approximately

$$\tau_{D;n} = h_- [1 + \ln(n-1)][1 + \sigma\alpha_T - 2\sqrt{\sigma\alpha_T}]^{-1}. \quad (E10)$$

REFERENCES

1. Oosawa, F., and M. Kasai. 1962. Theory of linear and helical agggregations of macromolecules. *J. Mol. Biol.* 4:10–21.
2. Oosawa, F., and S. Asakura. 1975. Thermodynamics of the Polymerization of Protein. Academic Press, Inc., NY.
3. Wegner, A., and J. Engel. 1975. Kinetics of the cooperative association of actin to actin filaments. *Biophys. Chem.* 3:215–225.
4. Wegner, A., and P. Savko. 1982. Fragmentation of actin filaments. *Biochemistry.* 21:1909–1913.
5. Korn, E. D. 1982. Actin polymerization and its regulation by proteins from nonmuscle cells. *Physiol. Rev.* 62:672–737.
6. Frieden, C. 1985. Actin and tubulin polymerization: the use of kinetic methods to determine mechanism. *Annu. Rev. Biophys. Biophys. Chem.* 14:189–210.
7. Heicklen, J. 1976. Colloid Formation and Growth: Chemical Kinetic Approach. Academic Press, Inc., NY.
8. Bentz, J., and S. Nir. 1981. J. Chem. Soc. Faraday Trans. 1. 77:1249–1275.
9. Hendriks, E. M., and M. H. Ernst. 1984. Exactly soluble addition and condensation models in coagulation kinetics. *J. Colloid Interface Sci.* 97:176–194.
10. Tobacman, L. S., and E. D. Korn. 1983. The kinetics of actin nucleation and polymerization. *J. Biol. Chem.* 258:3207–3214.
11. Frieden, C., and D. W. Goddette. 1983. Polymerization of actin and actin-like systems: evaluation of the time course of polymerization. *Biochemistry.* 22:5836–5843.
12. Bishop, M. F., and F. A. Ferrone. 1984. Kinetics of nucleation-controlled polymerization. *Biophys. J.* 46:631–644.
13. Newman, J., J. E. Estes, L. A. Selden, and L. C. Gershman. 1985. Presence of oligomers at subcritical actin concentrations. *Biochemistry.* 24:1538–1544.
14. Mozo-Villarias, A., and B. R. Ware. 1985. Actin oligomers below the critical concentration detected by fluorescence photobleaching recovery. *Biochemistry.* 24:1544–1548.
15. Oosawa, F. 1970. Size distribution of protein polymers. *J. Theor. Biol.* 27:69–86.
16. Pollard, T. D. 1984. Polymerization of ADP-actin. *J. Cell Biol.* 99:769–777.
17. Pantaloni, D., T. L. Hill, M. F. Carlier, and E. D. Korn. 1985. A model for actin polymerization and the kinetic effects of ATP hydrolysis. *Proc. Natl. Acad. Sci. USA.* 82:7205–7211.
18. Ferrone, F. A., F. Hofrichter, and W. A. Eaton. 1985. Kinetics of Sickle Hemoglobin Polymerization. *J. Mol. Biol.* 183:591–610.
19. Acton, F. S. 1970. Numerical Methods that Work. Harper and Row, NY, Evanston, London.
20. Ziman, J. M. 1972. Principles of the Theory of Solids. Cambridge University Press, Cambridge, London, New York, Melbourne.